

Intradot dynamics of InAs quantum dot based electroabsorbers

Tomasz Piwonski,¹ Jaroslaw Pulka,¹ Gillian Madden,¹ Guillaume Huyet,¹ John Houlihan,^{2,a)} Evgeny A. Viktorov,³ Thomas Erneux,³ and Paul Mandel³

¹Tyndall National Institute, Prospect Row, Cork, Ireland, and Department of Applied Physics, Cork Institute of Technology, Cork, Ireland

²Department of Computing, Maths, and Physics, Waterford Institute of Technology, Waterford, Ireland

³Université Libre de Bruxelles, Optique Nonlinéaire Théorique, Campus Plaine, Code Postal 231, 1050 Bruxelles, Belgium

(Received 16 January 2009; accepted 5 March 2009; published online 27 March 2009)

The carrier relaxation and escape dynamics of InAs/GaAs quantum dot waveguide absorbers is studied using heterodyne pump-probe measurements. Under reverse bias conditions, we reveal differences in intradot relaxation dynamics, related to the initial population of the dots' ground or excited states. These differences can be attributed to phonon-assisted or Auger processes being dominant for initially populated ground or excited states, respectively. © 2009 American Institute of Physics. [DOI: 10.1063/1.3106633]

The physics of quantum dot (QD) based optical devices has been studied intensively due to their interesting blend of atomic and solid state properties.¹ Recently, attention has been focused on their absorption properties and has led to QD materials finding favor in such applications as monolithic mode-locked lasers,² electroabsorption modulators,³ and saturable absorber mirrors.⁴ Time-resolved pump-probe spectroscopy is a very useful technique to investigate the fundamental timescales and underlying dynamical processes occurring in such absorbers; a notable example being the demonstration of the dynamical role of different carrier types for QW devices.⁵ More recently, similar techniques were applied to QD structures to explain the nature of tunneling processes at high reverse bias voltages⁶ and to demonstrate the electroabsorption properties of a bilayer QD waveguide.⁷

In this letter, the nonlinear recovery of QD based reversed-biased waveguide absorbers is analyzed using a single color pump-probe technique. Either the dots' ground state (GS) or excited state (ES) is initially populated thus increasing the transmission, and the resulting absorption recovery dynamics is recorded. The recovery dynamics is observed to be dependent on the initial population of the dots' energy states. The difference in recovery dynamics can be understood by the ES to GS carrier relaxation process being phonon assisted when the dots are initially populated in the GS, while it is Auger related when the dots' ES is initially populated.

In our experiments, we study intradot relaxation processes as a function of reverse bias using time-resolved spectroscopy. The QD waveguide absorber was 1 mm long, had 4 μm width ridges together with tilted, antireflection coated facets. It was fabricated from a material that included six stacks of InAs/GaAs QDs in a dots-in-a-well structure, grown by Zia Inc. (see Ref. 8 for further details of the material and experimental technique). To summarize, the GS and ES peaks appear at 1320 and 1250 nm, respectively. The pump-probe differential transmission was measured using a heterodyne detection technique. Pulses of about 600 fs width at either 1320 or 1250 nm were obtained from a titanium-sapphire pumped, optical parametric oscillator and split into three beams: reference, pump, and probe (260 fJ pump pulse

energy, 13 fJ probe pulse energy). After propagation through the waveguide absorber with suitable delays, the frequency shifted probe and reference beams were overlapped on a detector, and the amplitude of the difference frequency was detected using a high frequency lock-in amplifier. The resulting signal is proportional to the differential transmission ΔT of a probe pulse at the same wavelength as the pump. The resulting data, taken at room temperature, are normalized to the maximum differential transmission at zero reverse bias T_0 and therefore represented by $\Delta T/T_0$.

Figure 1 displays the normalized GS and ES relaxations for a range of reverse bias voltages. The two sets of time traces are very similar, both exhibiting a decrease in the relaxation time with increasing reversed bias voltage. However, one may notice that the relaxation of the ES generally occurs over a faster timescale compared to that of the GS. We shall demonstrate that this difference in recovery timescales together with the shape of the absorption recovery originates from a change in the dominant intradot relaxation process.

The experimental time traces can be classified into two groups depending on the reverse bias voltage. The recovery dynamics in the low voltage (0–4 V) group has two distinct stages of recovery: the fast (≈ 10 ps) and the slow (> 10 ps). For higher (5–9 V) reverse voltages, the recovery

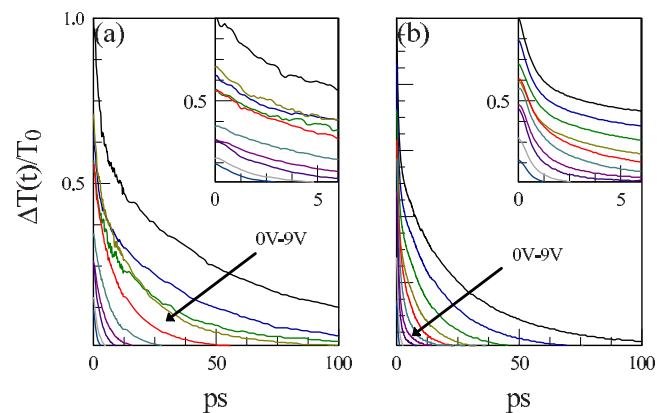


FIG. 1. (Color online) Differential transmission at (a) GS and (b) ES wavelengths at different reverse biased voltages. The dynamics in the (0–4 V) range consists of a two stage recovery. In the (5–9 V) range, a single stage recovery is present suggesting linear relaxation.

^{a)}Electronic mail: jhoulihan@wit.ie.

consists of only one fast stage (<10 ps) and the slow stage cannot be distinguished. The existence of the two ranges can be related to different processes contributing to the recovery. At high voltage, fast tunneling processes from the QD to adjacent layers become dominant and define the linear recovery. This effect was analyzed in Ref. 6. Therefore, we concentrate on the analysis of the two stage recovery that occurs in the low voltage range.

The model of QD carrier dynamics valid for the absorber is governed by equations for the occupation probabilities $\rho_{g,e}$ of the GS and the first ES of a dot

$$\partial_t \rho_g = -\tau^{-1} \rho_g + 2F(\rho_g, \rho_e), \quad (1)$$

$$\partial_t \rho_e = -\tau_w^{-1} \rho_e - F(\rho_g, \rho_e). \quad (2)$$

The factor 2 in Eq. (1) accounts for the spin degeneracy in the QD energy levels. $\tau \approx 1$ ns is the carrier recombination time in the dots. The function $F(\rho_g, \rho_e)$ is associated with the carrier exchange rate between the GS and ES in the dot. We assume that the reverse bias conditions do not allow recapturing from the wetting layer and model the relaxation from the ES to the wetting layer by the linear term $\tau_w^{-1} \rho_e$. This approximation may be limited for the unbiased case where recapturing from the wetting layer may also play a minor role. The parameter τ_w^{-1} is the carrier escape rate from the ES to the wetting layer and depends on the reverse bias. The functional dependence of τ_w on the reverse bias may be extracted by fitting the experimental data. As in Ref. 6, we do not include screening effects which are expected to be small for this material system.

The type of intradot relaxation which dominates the function $F(\rho_g, \rho_e)$, depends on the initial carrier density. In general, the energy exchange consists of only two types of interaction: phonon-assisted or Auger-type recombination. In both cases, the interaction is limited by Pauli blocking and so must be multiplied by a factor $(1-\rho)$. Phonon-assisted capturing depends only on the energy level spacing, and always contributes to relaxation processes in the InAs/GaAs structure. Auger processes become dominant when the carrier density in a particular state increases. Due to the increased number of first ESs compared with GSs, the absorption is greater for the ES than GS at a particular reversed bias voltage and thus Auger relaxation processes should be considered when pumping occurs in the ES.

Let us first examine the experimental data on GS relaxation. Pumping the GS induces a strong GS population and saturation of the GS. The ES is initially empty and never becomes strongly populated because of the very fast escape to the wetting layer. As a result, we can neglect Auger-like transitions and formulate the carrier exchange rate as

$$F(\rho_g, \rho_e) = \tau_{\text{cap}}^{-1} \rho_e (1 - \rho_g) - \tau_{\text{esc}}^{-1} \rho_g (1 - \rho_e), \quad (3)$$

where $1 - \rho_{g,e}$ is the Pauli blocking factor and τ_{cap}^{-1} , τ_{esc}^{-1} are the carrier capture and escape rates, respectively. We assume that $\rho_g(0) = \rho_0 \leq 1$ and depends on the reverse bias. We consider $\rho_e(0) = 0$ implying that initially there are no free carriers in the ES. The term $\tau_{\text{cap}}^{-1} \rho_e (1 - \rho_g)$ describes recapturing by the GS and is linearly proportional to the population of the ES. It corresponds to a phonon-assisted interaction.

The parameters τ_{cap} , τ_{esc} , and τ_w determine the time-dependent recovery of the QD absorber. In the low voltage range (0–4 V), we find that variations of τ_{cap} and τ_{esc} with

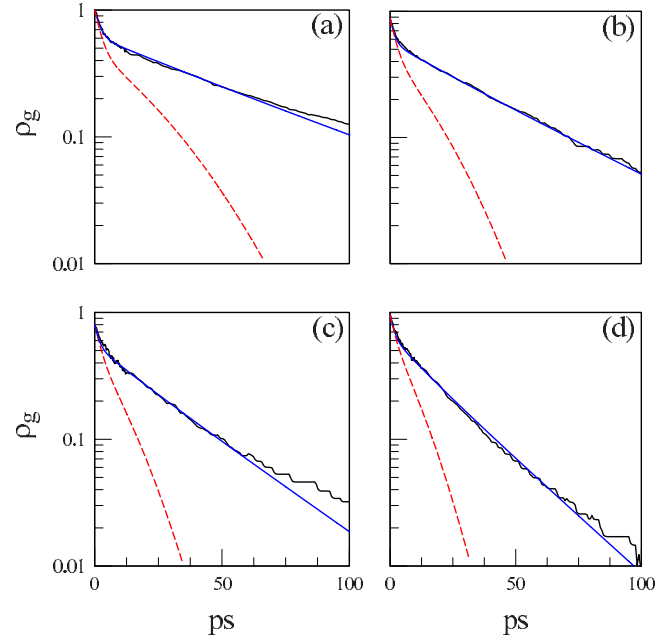


FIG. 2. (Color online) Experimental GS carrier relaxation for different reverse biased voltages (black) and fitting (blue) with Eqs. (1)–(3): (a) 0 V, $\tau_w=18$ ps, (b) 1 V, $\tau_w=12$ ps, (c) 2 V, $\tau_w=8$ ps, and (d) 3 V, $\tau_w=5$ ps. The other fitting parameters were $\tau_{\text{cap}}=2$ ps and $\tau_{\text{esc}}=10$ ps. The red (dashed) lines correspond to fitting with Auger-like ES to GS relaxation using Eq. (5).

voltage are negligible, and the dynamics of GS transmission can be reproduced by incorporating all of the voltage dependency into the carrier escape to the wetting layer τ_w .

To compare the experimental data to the model, we assume that $\Delta T(t)/T_0$ is proportional to the GS (ES) population of a dot and that the pump pulse completely populates the GS (ES) for zero voltage. This rescales the experimental data to $0 < \rho_{g,e}(t) < 1$ and results in a significant difference in $\rho_{g,e}(0)$ for different voltages. Fits of the experimental results to the theory are shown in Fig. 2. The fits show very good agreement with the experimental data for $\tau_{\text{cap}}=2$ ps and $\tau_{\text{esc}}=10$ ps. The corresponding values for τ_w as a function of voltage are shown in Fig. 3 and can be described by τ_w

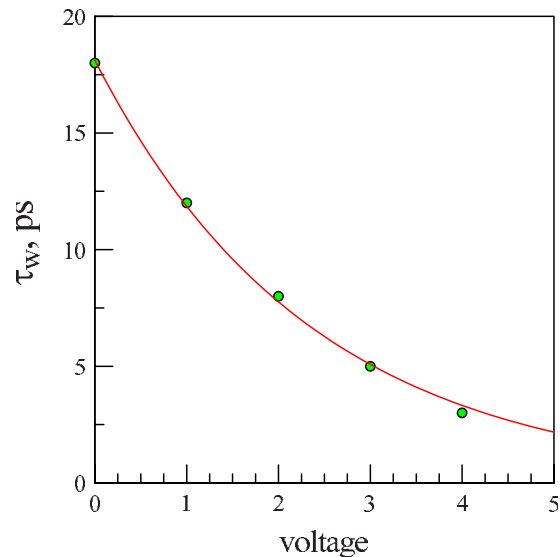


FIG. 3. (Color online) The parameter τ_w and its fitting to $\tau_w = \tau_{w0} \exp(-V/V_0)$ as a function of voltage V with $\tau_{w0}=18$ ps and $V_0=-2$ V.

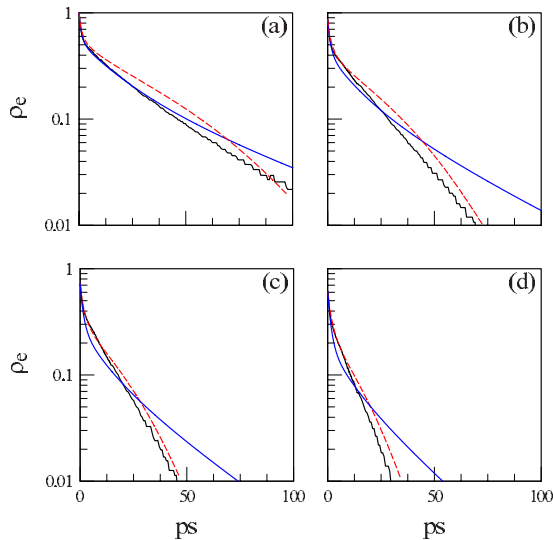


FIG. 4. (Color online) Experimental ES carrier relaxations (black) and fitting (red) with Eq. (5) for different voltages (0–3 V). $\tau_{\text{Auger}}=1.5$ ps. Other parameters are the same as in Fig. 2. The blue (solid) lines correspond to fitting with phonon-assisted relaxation using Eq. (3).

$=\tau_{w0} \exp(-V/V_0)$, where $\tau_{w0}=18$ ps and $V_0\approx-2$ V. Very similar results with $\tau_{w0}\approx 20$ ps were reported for the recovery of QW based structures⁹ and successfully used in the modeling.¹⁰ The exponential dependence on applied voltage results from a thermally activated rate process, as introduced in Ref. 11 A similar exponential variation of thermionic emission time with voltage ($V_0\approx-3.8$ V) was presented in Ref. 6 and related to the expected drop in barrier height with voltage.

In the higher voltage range (5–9 V), the escape to the wetting layer becomes very fast $\tau_w\leq 3$ ps, which results in $\rho_e(t)\approx 0$. Therefore, we have a linear approximation for the GS relaxation at high voltage

$$\partial_t \rho_g = -\tau^{-1} \rho_g - 2\tau_{\text{esc}}^{-1} \rho_g, \quad (4)$$

where the escape rate $2\tau_{\text{esc}}^{-1}\gg\tau^{-1}$ depends on the reverse bias and is indistinguishable from τ_w^{-1} in the frame of this approach. This linear approximation corresponds to the recently published results on fast tunneling.⁶

The energy exchange in Eq. (3) based on the phonon-assisted interactions between GS and ES explains the carrier relaxation in the case where the initial population is in the GS, but does not fit the experimental traces that result from pumping the ES. The difference is visible in Fig. 4 and suggests significant changes in the nature of intradot, carrier relaxation processes.

When pumping the ES, Auger-type recombination can play a role and must be included in the formulation of the energy exchange $F(\rho_g, \rho_e)$. As we will see from comparison with the experimental data, the recovery of the ES is much better described by the modified model

$$F(\rho_g, \rho_e) = \tau_{\text{Auger}}^{-1} \rho_e^2 (1 - \rho_g) - \tau_{\text{esc}}^{-1} \rho_g (1 - \rho_e), \quad (5)$$

where again, $1-\rho_{g,e}$ is the Pauli blocking factor and $\tau_{\text{Auger}}^{-1}, \tau_{\text{esc}}^{-1}$ are the Auger relaxation and phonon-mediated escape rates, respectively. We also assume that $\rho_e(0)=\rho_0\leq 1$ and depends on the reverse bias, and consider $\rho_g(0)=0$, implying that there initially is no free carriers in the GS.

In its simplest form, Auger relaxation can be described by a scattering process between two electrons in the ES and

a vacancy in the GS and therefore reads $\tau_{\text{Auger}}^{-1} \rho_e^2 (1-\rho_g)$.¹² Auger scattering usually involves carriers in conduction and valence bands and a real description would require taking into account the populations of many different levels. However, as these levels relax very quickly they may be adiabatically eliminated and the dynamics reduces to Eq. (5). The second term in the equation deals with subsequent phonon-assisted carrier escape from the GS to the ES (an Auger process whereby two electrons initially in the GS scatter, one up to the ES and the other down in energy, is impossible).

It is worth emphasizing that the phonon-assisted processes do not disappear completely from the ES to GS transfer, in the case of ES pumping, and may provide some corrections. However, the dominant role of Auger recombination in the carrier dynamics is obvious in Fig. 4. The best fits appear for $\tau_{\text{Auger}}=1.5$ ps and for the same functional dependence of the escape to the wetting layer, on the voltage, i.e., $\tau_w=\tau_{w0} \exp(-V/V_0)$. For completeness, the Auger-mediated ES to GS carrier relaxation model was also applied to the GS pump-probe situation. However, as can be seen in Fig. 2, it does not reproduce the experimental behavior.

In conclusion, we have presented detailed measurements of the absorption recovery of a QD waveguide absorber. We have studied the GS and ES recoveries as a function of reverse bias voltage. Fitting the experimental results with a simple rate equation model for the intradot carrier dynamics, we have concluded that Auger-mediated recovery dominates if the device is pumped at the ES while phonon-mediated recovery dominates if the GS is pumped. This provides opportunities for the design of the next generation of electro-absorbing devices based on QD materials.

The authors would like to acknowledge informative discussions with Stephen Hegarty and Bob Manning. This study has been supported by Science Foundation Ireland under Contract No. SFI 07/IN.1/1929, the INSPIRE Programme, funded by the Irish Government's Programme for Research in Third Level Institutions, Cycle 4, National Development Plan 2007-2013, and the Institute of Technology Ireland's Strand I Programme. The authors in Bruxelles acknowledge the support of the Fonds National de la Recherche Scientifique (Belgium).

¹D. Bimberg, *J. Phys. D* **38**, 2055 (2005).

²M. G. Thompson, C. Marinelli, Y. Chu, R. L. Sellin, R. V. Penty, L. H. White, M. Van Der Poel, D. Birkedal, J. Hvam, V. M. Ustinov, M. Lammlin, and D. Bimberg, *Proceedings of the 19th IEEE International Semiconductor Laser Conference* (IEEE, New York, 2004) pp. 53–54.

³Y. Chu, M. G. Thompson, R. V. Penty, I. H. White, and A. R. Kovsh, *CLEO/QELS OSA Technical Digest* (Optical Society of America, Washington, DC, 2007), p. CMP4.

⁴D. J. H. C. Maas, A. R. Bellancourt, M. Hoffman, B. Rudin, Y. Barbarin, M. Golling, T. Sudmeyer, and U. Keller, *Opt. Express* **16**, 18646 (2008).

⁵J. A. Cavailles, D. A. B. Miller, J. E. Cunningham, P. L. K. Wa, and A. Miller, *IEEE J. Quantum Electron.* **28**, 2486 (1992).

⁶D. B. Malins, A. Gomez-Iglesias, S. J. White, W. Sibbett, A. Miller, and E. U. Rafailov, *Appl. Phys. Lett.* **89**, 171111 (2006).

⁷D. Malins, A. Gomez-Iglesias, P. Spencer, E. Clarke, R. Murray, and A. Miller, *Electron. Lett.* **43**, 686 (2007).

⁸T. Piwonski, I. O'Driscoll, J. Houlihan, G. Huyet, R. Manning, and A. Uskov, *Appl. Phys. Lett.* **90**, 122108 (2007).

⁹H. Yokoyama, *IEICE Trans. Electron.* **E85**, 2736 (2002).

¹⁰J. Mulet and J. Mork, *IEEE J. Quantum Electron.* **42**, 249 (2006).

¹¹G. Vincent, A. Chantre, and D. Bois, *J. Appl. Phys.* **50**, 5484 (1979).

¹²A. V. Uskov, Y. Boucher, J. L. Bihan, and J. McInerney, *Appl. Phys. Lett.* **73**, 1499 (1998).